PROCEEDINGS

55. IWK

Internationales Wissenschaftliches Kolloquium
International Scientific Colloquium

13 - 17 September 2010

Crossing Borders within the ABC

Automation,

Biomedical Engineering and

Computer Science

Faculty of
Computer Science and Automation

www.tu-ilmenau.de

TECHNISCHE UNIVERSITÄT
ILMENAU

Impressum
Published by

Publisher:	Rector of the Ilmenau University of Technology Univ.-Prof. Dr. rer. nat. habil. Dr. h. c. Prof. h. c. Peter Scharff
Editor:	Marketing Department (Phone: +49 3677 69-2520) Andrea Schneider (conferences@tu-ilmenau.de) Faculty of Computer Science and Automation (Phone: +49 3677 69-2860) Univ.-Prof. Dr.-Ing. habil. Jens Haueisen
Editorial Deadline:	20. August 2010
Implementation:	Ilmenau University of Technology Felix Böckelmann Philipp Schmidt

USB-Flash-Version.

Publishing House:	Verlag ISLE, Betriebsstätte des ISLE e.V. Werner-von-Siemens-Str. 16 98693 Ilmenau
Production:	CDA Datenträger Albrechts GmbH, 98529 Suhl/Albrechts
Order trough:	Marketing Department (+49 3677 69-2520) Andrea Schneider (conferences@tu-ilmenau.de)

ISBN: 978-3-938843-53-6 (USB-Flash Version)

Online-Version:

Publisher:	Universitätsbibliothek Ilmenau ilmedia Postfach 10 05 65 98684 Ilmenau

Home / Index:
http://www.db-thueringen.de/servlets/DocumentServlet?id=16739

SPECTRAL PATTERN CLASSIFICATION IN OPTICAL COHERENCE TOMOGRAPHY

Hubert Welp,[2] Volker Jaedicke,[1,2] Christoph Kasseck,[1] Nils C. Gerhardt[1], Martin R. Hofmann[1]

[1]Photonics and Terahertz Technology, Ruhr-University Bochum, Universitaetsstrasse 150, 44780 Bochum, Germany

[2]Department for Electrical and Electronic Engineering, University of Applied Sciences Georg Agricola, Herner Strasse 45, 44787 Bochum, Germany

ABSTRACT

In optical coherency tomography (OCT) several approaches are pursued to retrieve depth dependent spectroscopic information from the analysis of the backscattered light. Since many substances in life science and material science have characteristically shaped spectral extinctions in principle this allows depth dependent substance identification.

We present a concept using a pattern recognition algorithm to perform depth resolved substance identification in non-scattering samples based on spectral features. A proof of principle is given by frequency domain OCT (FD-OCT) measurements of a multilayer sample with four different absorbers.

For this sample we achieved an overall efficiency of 83% in identifying the different substances. This result was achieved without any calibration and correction of systematic errors.

Our proof of principle outlines the potential of spectral feature based substance identification with OCT at least in absorbing, non scattering samples e.g. for material sciences.

Index Terms – Optical Coherence Tomography (OCT), Spectroscopy, Pattern Recognition, Absorption

1. INTRODUCTION

In recent years, Optical Coherence Tomography (OCT) has become a standard non-invasive three dimensional imaging technique, especially for biomedical applications as in ophthalmology or dermatology. It provides high-resolution, cross-sectional images of scattering media such as biological tissues. It is noteworthy that OCT is especially qualified for medical applications, because it represents an imaging method, based on non-ionizing, harmless light radiation typically in the near-infrared wavelength range.

OCT is an interferometric technique to measure the backscattered light from different depths of a sample. There are a number of different OCT techniques. The two main categories are time-domain OCT (TD-OCT) and frequency-domain OCT (FD-OCT), whereas the latter has been claimed to be the more sensitive method [3]. For more details on the principles, techniques and applications of OCT see [1].

Currently there are several approaches to retrieve not only morphological information from the analysis of the backscattered light but also depth dependent spectroscopic information, called spectroscopic OCT (SOCT). SOCT provides additional tissue information in tomographic images obtained by FD-OCT [2] or TD-OCT systems [3]. Furthermore depth resolved spectroscopic analysis in FD-OCT is divided into two main analysis principles. The first one uses systems with different wavelength bands. The resulting images can be compared to each other in a differential color encoded image [4]. The second principle utilizes windowed Fourier transform in the frequency or spatial regime [5][6][7][8]. In general, both principles provide additional contrast by analyzing spectroscopic information in addition to pure backscattering information. The spectral or spatial windowing approach also enables recalculating the spectra from different depths and therefore offers access to the spectral modifications of each layer. Recently Kartakoullis et al. applied spectral estimation and pattern recognition techniques on TD-SOCT signals to distinguish scattering particles of different sizes [9]. Their approach is based on wavelength dependent scattering using a central wavelength of 1250 nm.

We present a concept using a pattern recognition algorithm to identify substances by their absorption characteristics. This is done in the wavelength regime from 750nm to 1000nm where many substances in biological tissues and material sciences show characteristic absorptions.

2. CONCEPT

In the following our image analysis concept for the extraction of spectroscopic information from FD-OCT data with subsequent depth dependent substance identification is depicted roughly. Further details on the single analysis steps are given in chapter 4.

The standard FD-OCT image, obtained by an inverse Fourier transform from the measured spectral

data, is generated with the full depth resolution. This is not limited by the subsequent spectroscopic image analysis. In this analysis, a region of interest in the depth profile is Fourier transformed. This provides the backscattered spectrum of the corresponding depth area. By sequentially analyzing subsequent peaks in the depth profile, spectral modifications from different layers can be calculated by using the squared division of two spectra from adjacent peaks. These spectral power transfer functions can be used for tissue identification by means of a pattern recognition algorithm. Here, the transfer functions are classified into classes of known absorption profiles of expected substances. In a last step the standard FDOCT image is coloured according to the recognised substances.

Thus, precise spectroscopic reconstruction is possible with laterally and depth resolved substance identification. As a side effect the image contrast is increased by the superposed spectroscopic colour map onto the inverse grey scale map from the standard FD-OCT image.

3. EXPERIMENTAL SETUP

To perform proof-of-principle measurements on phantom samples we used a standard FD-OCT system as depicted in Figure 1a, which is basically a free beam Michelson interferometer. A photonic crystal fiber based supercontinuum light source (Koheras SuperK Versa) supplies the setup with a white light spectrum. The superimposed beams from the reference mirror and the sample are coupled into a single mode fiber that guides the interfering light into an optical spectrum analyzer (OSA). The measurements were performed in the range from 750nm to 1000nm. All optical components were matched to this wavelength range.

The phantom sample consisted of three different colour glass filters (Schott RG830, RG850 and BG36) and a neutral density filter (Schott NG12). The filters were arranged in two layers with an air gap of 200µm in between, as shown in Figure 1b. The thickness of the filters was 600µm each. Furthermore a reference sample with the same layout and the same dimensions consisting only of neutral density filters (Schott NG12) was used for calibration purposes.

4. METHODS AND RESULTS

In this chapter we will 1) explain our algorithm to reconstruct the transmission spectra of a sample layer (called *transfer functions*) from the FD-OCT data, 2) provide experimental results showing the validity of our concept to extract spectral transfer functions and 3) present an image analysis algorithm that is based on spectral pattern recognition and provides reliable, depth resolved substance identification.

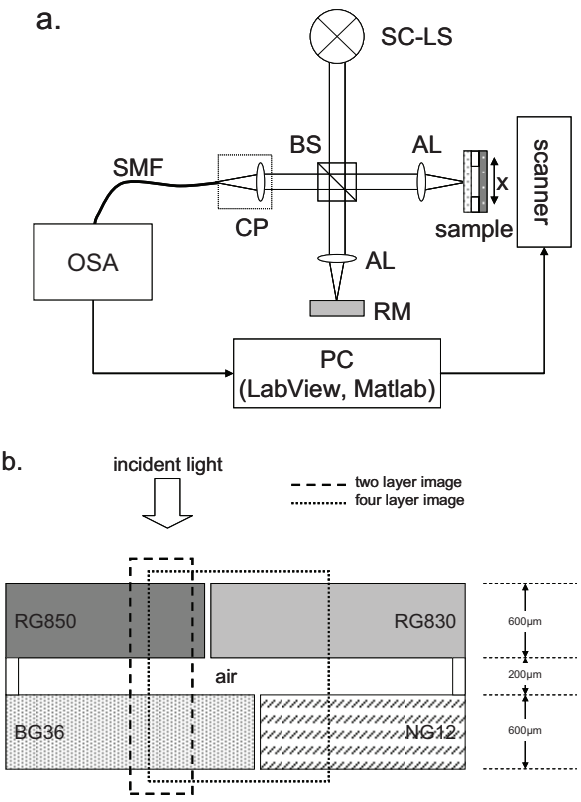

Figure 1 (a.) Experimental setup. SC-LS: super continuum light source, BS: beam splitter, AL: achromatic lenses, RM: reference mirror, CP: collimation package, SMF: single mode fiber, OSA: optical spectrum analyzer, PC: personal computer (b.) Sketch of the used phantom sample consisting of glass filters. The dashed and dotted lines show the different images taken with the FD-OCT setup above.

4.1. Spectral data extraction algorithm

Our spectral data extraction algorithm is based on the idea that a single peak in the depth profile of an OCT image is a convolution of a delta function and the spectrum of the backscattered light from the corresponding depth region (Figure 2). Thus a windowed Fourier transform of the peak directly yields the desired spectrum. For more details see [10].

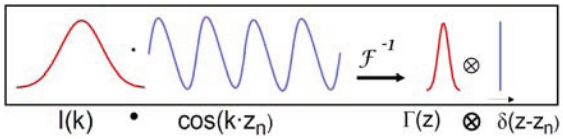

Figure 2 I(k): Spectrum of the backscattered light, cos(kz_n): Modulation, Γ(z): Fourier transform of I(k), δ: Fourier transform of cos(kz_n), k: wave number, z: depth, z_n:depth of n-th layer

The main steps to reconstruct individual transfer functions are shown in the block diagram of Figure 3. In detail the analysis procedure looks as follows. 1) The measured FD-OCT spectrum is resampled into the k-space.

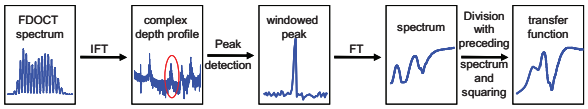

Figure 3 Block diagram of spectral data extraction procedure.

2) Then this resampled spectrum is inverse Fourier transformed yielding the complex depth profile as used for standard OCT images. 3) To identify reflecting surfaces in the sample peaks in the depth profile are determined on a threshold basis. 4) A depth interval around these peaks is cut out, smoothed by either a Kaiser or Blackman window and zero padded to the original number of data points. 5) A subsequent Fourier transform of this depth interval provides the spectrum of the backscattered light from this region. 6) In order to retrieve the transfer functions of a sample layer the spectra of two adjacent peaks are divided by each other, squared and resampled back into the wavelength space.

The whole algorithm was integrated into a single MATLAB program with a user friendly graphical user interface. It allows the user to select the values of a variety of parameters for the analysis procedure like e.g. the interval width or the peak threshold.

To validate our concept we implemented a numerical simulation of the FD-OCT setup. The simulation provides simulated detector signals for simulated samples. This signal can be used as an input for our analysis algorithm. The simulation used a sum of interfering waves with different frequencies. The propagation through the FD-OCT setup is calculated separately for the individual waves according to the linearity of the system. The spectrum of the light source and the influence of the transmission characteristic of a sample layer were simulated by setting the amplitudes of the individual waves accordingly.

Figure 4 shows reconstructed transfer functions derived with our algorithm from simulated input signals. The left figure shows the result for a simulated sample consisting of a layer with a rectangular transmission function. In the right figure a much smoother transmission was chosen, similar to those of glass filters. In both cases the reconstructed transfer functions agree very well with the input transmission functions, confirming the validity of the analysis concept. The deviations in the first example and at the edges at 1000nm in the second example are due the limited spectroscopic resolution. With an interval width of only 50 data points, as used in this analysis, the spectroscopic resolution is not sufficient to reconstruct such unnatural steep courses in the curves.

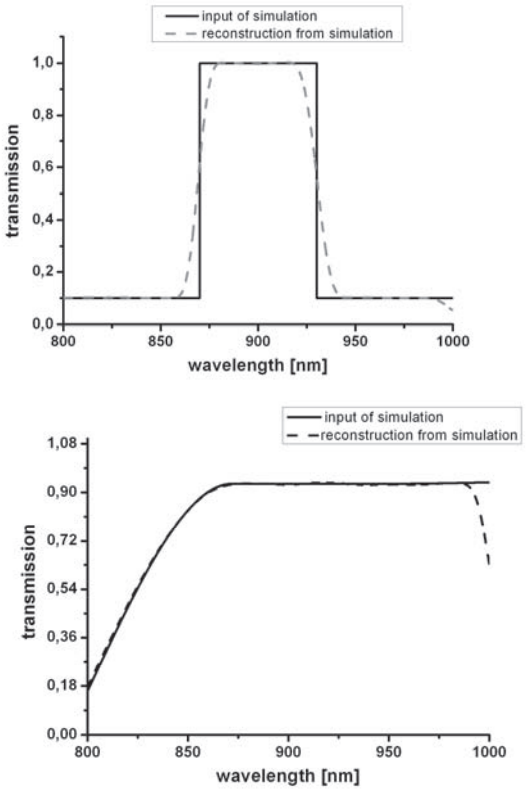

Figure 4 : Reconstructed transfer functions derived from simulated FD-OCT signals of different simulated samples.

4.2. Experimental results

To verify the spectral data extraction algorithm with real FD-OCT data two different images were taken from the multilayer sample shown in Figure 1b. A two-layer-image spans an area with two filters (RG850, BG36) and a four-layer-image spans an area with all four filters.

Figure 5 and Figure 6 show the results for the two-layer-image. The solid curves represent the transmission spectra of the corresponding filters. These spectra were measured separately to serve as a comparison standard for the transfer functions reconstructed from the FD-OCT data. The reconstructed transfer functions are displayed with dotted lines. All curves show only minor deviations demonstrating the capability of our concept to perform depth resolved spectroscopic analysis for FD-OCT with high precision.

The transfer functions in Figure 5 and Figure 6 were derived as follows. The two layer image consists of 100 depth profiles with a lateral step width of 10µm in between. The depth resolved spectral characteristics of the two layer image were reconstructed as described in chapter 4.1.

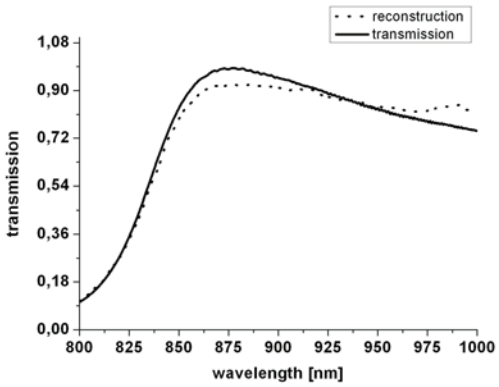

Figure 5 : Reconstructed transfer function of the RG850 filter in the top layer.

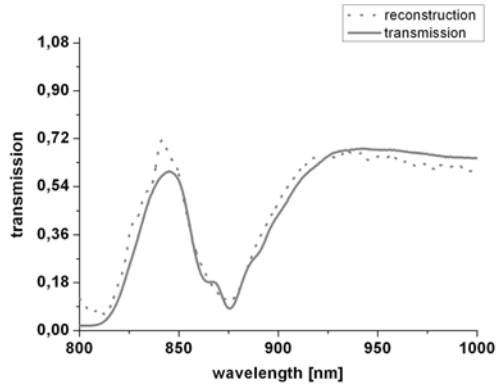

Figure 6 : Reconstructed transfer function of the BG36 filter in the bottom layer.

The spectroscopic analysis of the two layer image with four strong backscattering boundaries is resulting in a set of three reconstructed spectral power transfer functions for RG850, air and BG36. To obtain smooth layer characteristics, the reconstructed data were averaged over seven depth profiles. The FD-OCT system itself has a wavelength dependent transfer characteristic which turned out to be even depth dependent and is most probably caused by chromatic aberration. Chromatic aberration is an inherent problem of SOCT setups and is reported by other groups as well [5]. This systematic error was quantified by measuring and reconstructing the transfer functions of the reference sample. The high accuracy of the reconstruction process shown in Figure 5 and Figure 6 could only be achieved by correcting the transfer functions of the filters with those of the reference sample.

4.3. Spectral pattern classification

The spectral information contained in the transfer functions has to be evaluated and visualized in a meaningful manner. A simple approach is to extract a single value out of the transfer function like e.g. the center of mass of the spectrum [3] or the full width of half maximum of the autocorrelation function of the spectrum [11]. Then this value can be color encoded and superimposed onto the standard OCT cross sectional image. This approach visualizes spectral modifications but is not very specific and does not guarantee that the relevant information is revealed, especially if the transfer functions are subject to considerable systematic or stochastic errors. A more ambitious approach is to interpret the transfer function as the spectral fingerprint of the substances contained in the sample by which they can be identified. The allocation of reconstructed transfer functions to classes of known transmission spectra and thus to substances is a typical pattern classification problem. This approach promises to provide much more meaningful, contrast enhanced OCT images and – because of its fault tolerance – possibly without the need for calibration with a reference sample. For real applications the construction of a reference sample is not feasible.

We have implemented a pattern recognition algorithm to analyze the transfer functions of the two-layer- and the four-layer-image of the phantom sample in Figure 1b. First, the **uncorrected** transfer functions were preprocessed by cutting off the edges and carrying out normalization. In principle each of the 50 discrete values of the transfer functions could serve as a feature in a classification process. To reduce the quantity of features and extract only the relevant information a Principal Component Analysis (PCA) was performed thus increasing the performance of the subsequent classification. The classification of the transfer functions was made in one of the four classes RG850, RG830, BG36 and air or NG12 respectively representing the known substances. Different classification methods were tested: Naive Bayes, discriminant function and classification tree.

A dataset of 2570 transfer functions from 14 different measurements was used to train and test the classifier. For this purpose the dataset was divided into a training dataset and a test dataset. The training dataset comprises 70% of the transfer functions and the test dataset 30%. In order to compare the different classifiers we used the following evaluation criteria (where applicable): efficiency, sensitivity, specificity and area under receiver operating characteristic curve (AU ROC).

The table in Figure 7 shows the results. The number of principal components (PC) was tuned to maximize the performance of the respective classification method. E.g. with a Bayes classifier the best performance concerning the overall efficiency (total number of true positive divided by total number of transfer functions) was achieved with 8 principal components. This yields an efficiency of 83% in identifying the different substances.

In order to visualize the results from the spectral pattern classification process in the cross-sectional images we assigned each class or substance a certain colour. Figure 8 shows the four layer image of our phantom sample as a standard FD-OCT cross-sectional grey-scaled image. This image consists of

100 depth profiles with a step width of 30µm in between. It only shows the backscattering boundaries of the filters. It is not possible distinguish between the different filter types or air layers. The white crosses mark the peaks automatically detected by the software as boundaries. The weaker autocorrelation peaks are suppressed and not taken into account for the spectroscopic analysis. Figure 9 shows the same image with superimposed substance information derived from a spectral pattern classification analysis with a Bayes classifier. In the figure red represents the filter RG830, turquoise BG36 and green RG850. Areas where the classifier recognized air or the filter NG12 were not colored. In this image the different filters are clearly recognizable. All regions are colored quite homogenously showing the low error rate of the classifier.

Both the numerical results as well as the spectroscopically enhanced OCT-images demonstrate the feasibility to identify substances in different depth regions of non-scattering phantoms by their spectroscopic fingerprint. The decisive advantage of using pattern recognition techniques is that it makes a calibration with a reference sample unnecessary.

5. SUMMARY AND DISCUSSION

We present a spectroscopic analysis concept for identifying substances in conventional FD-OCT images of non-scattering samples. The concept comprises an algorithm to reconstruct depth resolved spectroscopic transfer functions and a spectral pattern classification algorithm to identify substances by their spectroscopic fingerprint. Our post processing image analysis software integrates all the necessary steps: depth profile calculation, peak detection, extraction of depth resolved spectra and reconstruction of transfer functions, feature extraction, classification and coloring of the standard OCT image according to the classification results. A proof-of-principle was given with a multi-layer phantom sample consisting of glass filters. It impressively demonstrates the ability of our approach to reconstruct depth resolved spectral information in absorbing media with high precision and recognizing substances even for systematically or stochastically disturbed transfer functions i.e. without calibration measurements. Besides the improved contrast the resulting images provide significant higher information content than conventional OCT images.

Our main interest for the application of spectroscopic OCT is focused on biological tissues. A possible application could be the distinction of carcinogenic from healthy skin in vivo. In order to deal with such problems we have to address three major challenges.

First, biological tissue is a strongly scattering media. We have to enhance our concept to separate the absorptive from the scattering contributions in the extracted spectral signal. There are successful approaches of other groups addressing this problem [12]. Scattering leads to characteristic spectral patterns providing additional information about the sample e.g. the size of the scatterers [14]. Other groups already analyzed this information e.g. to detect cancerous cells in hamster cheek [13].

Second, the structure detection in the image analysis software has to be improved for two reasons. 1) In biological tissues edges of different layers cannot be detected as easily as in our phantom sample. More sophisticated algorithms are needed to identify backscattering peaks and thus provide the starting points for our spectral analysis. 2) Generally in biomedical applications the highlighting of morphological information is necessary to simplify the interpretation of OCT images. We already started to

	Bayes	Discriminant function	Classification tree
#PCA	8	14	14
Efficiency	0,8333	0,7874	0,8766
Sensitiviy	0,7975	0,7154	0,8626
Specificity	0,9574	0,9460	0,9688
AU-ROC	0,9597	0,9668	%

Figure 7 : Results for the classification of transfer functions into classes of different filter types.

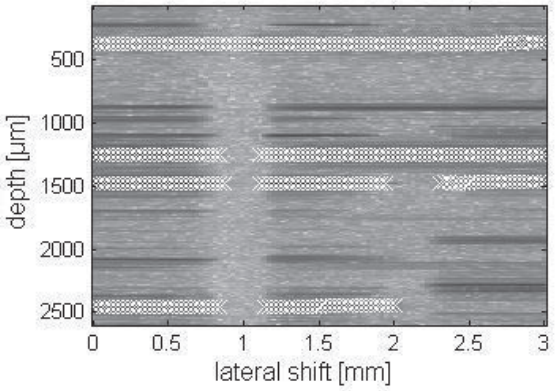

Figure 8 : Standard FD-OCT image of the four layer sector of the phantom sample. White crosses: peaks detected by the analysis software.

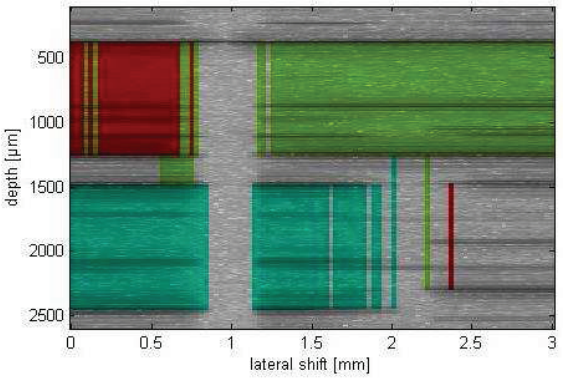

Figure 9: Four layer image enhanced with substance information derived with a Bayes classifier.

integrate a more intelligent edge detection algorithm into our image analysis software. Figure 10 shows a conventional OCT image of a human skin sample with highlighted edges. To detect the edges in a first step the original cross-sectional image is converted to a binary image. Optionally the binary image can be smoothed with a median- or Wiener filter. In a last step one of the different edge filters Roberts, Sobel, Prewitt, Canny or LoG (Laplacian of Gaussian) can be selected to ultimately detect the edges.

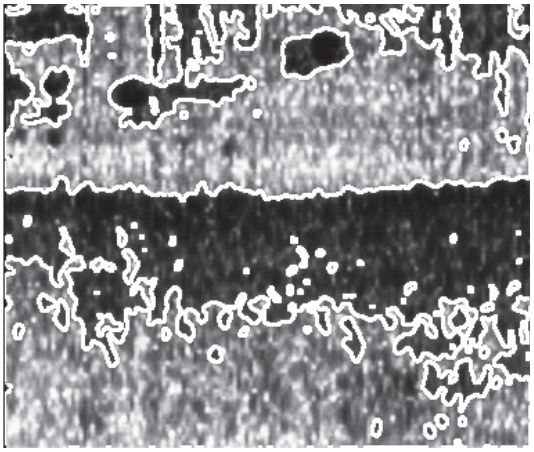

Figure 10: OCT image of human skin with edge detection.

Third, the FD-OCT experimental setup has to be improved. The systematic error caused by chromatic aberration has to be reduced or otherwise compensated to make the classification algorithm more robust. Furthermore, the overall performance of the system with respect to lateral resolution, sensitivity and data acquisition and processing speed has to be increased as well.

Acknowledgements: We thank the Stiftung Rheinisch-Westfälischer Technischer Überwachungs-verein (RWTÜV) for financial support.

6. REFERENCES

[1] B. E. Bouma and G. J. Tearney (Eds.), "Handbook of Optical Coherence Tomography", Dekker, New York, 2002

[2] R. Leitgeb, M. Wojtkowski, A. Kowalczyk, C. K. Hitzenberger, M. Sticker, A. F. Fercher, "Spectral measurement of absorption by spectroscopic frequency-domain optical coherence tomography," Opt. Lett. 25, pp. 820–822, 2000

[3] U. Morgner, W. Drexler, F. X. Kärtner, X. D. Li, C. Pitris, E. P. Ippen,, J. G. Fujimoto, "Spectroscopic optical coherence tomography," Opt. Lett. 25, pp. 111–113, 2000

[4] S. Kray, F. Spöler, M. Först, Heinrich Kurz, "High-resolution simultaneous dual-band spectral domain optical coherence tomography," Opt. Lett. 34, pp. 1970-1972, 2009

[5] B. Hermann, B. Hofer, C. Meier, W. Drexler, "Spectroscopic measurements with dispersion encoded full range frequency domain optical coherence tomography in single- and multilayered non–scattering phantoms," Opt. Express 17, pp. 24162-24174, 2009

[6] A. L. Oldenburg, C. Xu, S. A. Boppart, "Spectroscopic Optical Coherence Tomography and Microscopy," IEEE J. Sel. Top. Quantum Electron. 13, pp. 1629–1640, 2007

[7] A. Wax, C. Yang, J. A. Izatt, "Fourier-domain low coherence interferometry for light-scattering spectroscopy", Opt. Lett. 28, pp. 1230-1232, 2003

[8] C. Xu, C. Vinegoni, T. S. Ralston, W. Luo, W. Tan, S. A. Boppart, "Spectroscopic spectral-domain optical coherence microscopy," Opt. Lett. 31, pp. 1079-1081, 2006

[9] A. Kartakoullis, E. Bousi, C. Pitris, "Scatterer size-based analysis of optical coherence tomography images using spectral estimation techniques", Opt. Express 18, pp. 9181-9191, 2010

[10] Christoph Kasseck, Volker Jaedicke, Nils C. Gerhardt, Hubert Welp, Martin R. Hofmann, "Substance identification by depth resolved spectroscopic pattern reconstruction in frequency domain optical coherence tomography", Optics Communications, 2010 (accepted)

[11] D. Adler, T. Ko, P. Herz, J. Fujimoto, "Optical coherence tomography contrast enhancement using spectroscopic analysis with spectral autocorrelation," Opt. Express 12, pp. 5487-5501, 2004

[12] C. Xu, D. Marks, M. Do, S. Boppart, "Separation of absorption and scattering profiles in spectroscopic optical coherence tomography using a least-squares algorithm," Opt. Express 12, pp. 4790-4803, 2004

[13] Graf, Robles, Chen, Wax, "A Detecting precancerous lesions in the hamster cheek pouch using spectroscopic white-light optical coherence tomography to assess nuclear morphology via spectral oscillations", JOURNAL OF BIOMEDICAL OPTICS, 2009

[14] C. Xu, P. Carney, S. Boppart, "Wavelength-dependent scattering in spectroscopic optical coherence tomography," Opt. Express 13, ppl. 5450-5462, 2005